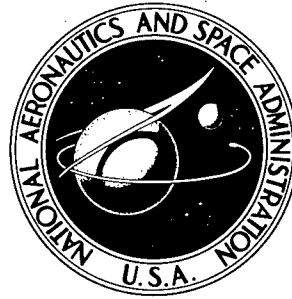


NASA TECHNICAL NOTE



NASA TN D-2331

NASA TN D-2331

PROPERTY OF:
AMPTIAC LIBRARY

57442

DISTRIBUTION STATEMENT A
Approved for Public Release
Distribution Unlimited



FATIGUE-CRACK PROPAGATION
IN SEVERAL TITANIUM AND
STAINLESS-STEEL ALLOYS
AND ONE SUPERALLOY

REPRODUCED FROM
BEST AVAILABLE COPY

by C. Michael Hudson
Langley Research Center
Langley Station, Hampton, Va.

20010906 131

FATIGUE-CRACK PROPAGATION IN SEVERAL
TITANIUM AND STAINLESS-STEEL ALLOYS AND ONE SUPERALLOY

By C. Michael Hudson

Langley Research Center
Langley Station, Hampton, Va.

NATIONAL AERONAUTICS AND SPACE ADMINISTRATION

For sale by the Office of Technical Services, Department of Commerce,
Washington, D.C. 20230 -- Price \$0.75

FATIGUE-CRACK PROPAGATION IN SEVERAL

TITANIUM AND STAINLESS-STEEL ALLOYS AND ONE SUPERALLOY

By C. Michael Hudson

SUMMARY

Axial-load fatigue-crack-propagation tests were conducted on 8-inch-wide (20.3-cm) sheet specimens made of Ti-4Al-3Mo-1V (Aged), Ti-6Al-4V (Annealed), and Ti-8Al-1Mo-1V (Triplex Annealed) titanium alloys, AM 350 (20-percent CR), AM 350 (Double Aged), PH 14-8Mo (SRH 950), PH 15-7Mo (TH 1050), and AISI 301 (50-percent CR) stainless steels, and Rene 41 (Condition B). Tests were run at 80° F (300° K), 550° F (561° K), and, in some cases, -109° F (195° K) to determine the effect of temperature on the fatigue-crack-propagation characteristics of each material. *Fatigue crack-propagation curves are presented.*

The materials are ranked according to their resistance to fatigue-crack propagation, and Ti-8Al-1Mo-1V (Triplex Annealed) appeared to be the most resistant over the temperature range of the investigation.

Special apparatus developed for the elevated- and cryogenic-temperature studies are described herein.



INTRODUCTION

The elevated temperatures associated with aircraft flying at a Mach number of approximately 2.5 and faster precludes the use of aluminum alloys for structural components. Consequently, aircraft designers must turn to more heat-resistant materials with which they have had little aircraft-design experience. Important to the selection of these materials is their resistance to fatigue-crack propagation and the effect of temperature on this resistance. Designers know that fatigue cracks will probably form in their aircraft structures, and consequently they must select materials having high resistance to crack growth in order to minimize the danger of fatigue failure.

An investigation has been undertaken to evaluate the crack-propagation characteristics of nine materials suitable for use at elevated temperatures. This investigation included tests of the nine materials at room temperature of 80° F (300° K) and at elevated temperature of 550° (561° K). To evaluate further the effects of temperature on fatigue-crack growth, two of the materials were

tested at the cryogenic temperature of -109° F (195° K). Tests have been conducted at positive mean stresses on sheet specimens made of five stainless steels, three titanium alloys, and one superalloy.

The present paper presents the experimental results of this study. Included are effects of temperature on crack propagation in each material and a relative ranking of each material with respect to resistance to crack growth at each test temperature.

SYMBOLS

All physical properties in this paper are given in both U.S. Customary Units and the International System of Units. An appendix is included to explain the relationship between the two systems.

E	Young's modulus, ksi or giganewtons/meter ² (GN/m ²)
e	total elongation in 2-inch-(5.08-cm) gage length, percent
N	number of cycles
R	ratio of minimum stress to maximum stress
S _a	alternating stress amplitude, ksi or meganewtons/meter ² (MN/m ²)
S _m	mean stress, ksi or meganewtons/meter ² (MN/m ²)
σ _u	ultimate tensile strength, ksi or meganewtons/meter ² (MN/m ²)
σ _y	yield strength (0.2-percent offset), ksi or meganewtons/meter ² (MN/m ²)
x	one-half of total length of central symmetrical crack, inches or centimeters (cm)

SPECIMENS AND TESTS

Specimens

The five stainless steels, three titanium alloys, and one superalloy studied in this investigation are listed as follows:

AISI 301 (50-percent Cold Rolled - CR)

AM 350 (20-percent Cold Rolled and Tempered - CRT)

AM 350 (Double Aged - DA)

PH 15-7Mo (TH 1050)

PH 14-8Mo (SRH 950)

René 41 (Condition B)

Ti-8Al-1Mo-1V (Triplex Annealed)

Ti-6Al-4V (Annealed)

Ti-4Al-3Mo-1V (Aged)

All the material for each alloy was obtained from the same mill heat. The heat treatment or rolling condition for each material is listed in table I. The tensile properties are listed in table II, and the nominal chemical composition of each material is listed in table III. The specimen configuration used is shown in figure 1. Sheet specimens 24 inches long (61 cm) and 8 inches wide (20.3 cm)

were used. Nominal thicknesses were 0.024 inch (6.10 mm) for the stainless steel and the superalloy and 0.040 inch (1.016 mm) for two of the titanium alloys and 0.050 inch (1.270 mm) for the third. All specimens were fabricated so that the longitudinal axis of the specimen was parallel to the grain of the sheet. In addition, standard ASTM tensile specimens were made from each sheet to determine tensile properties.

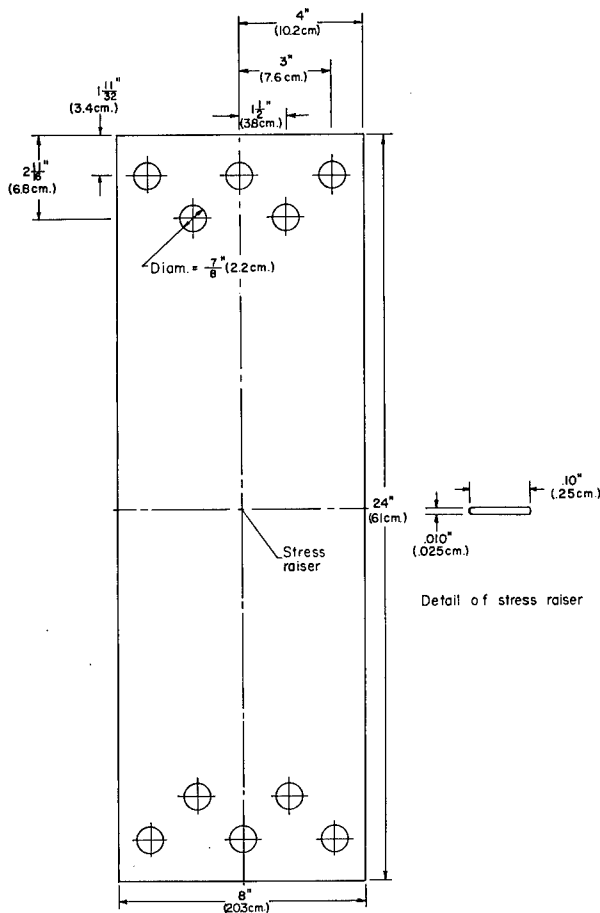


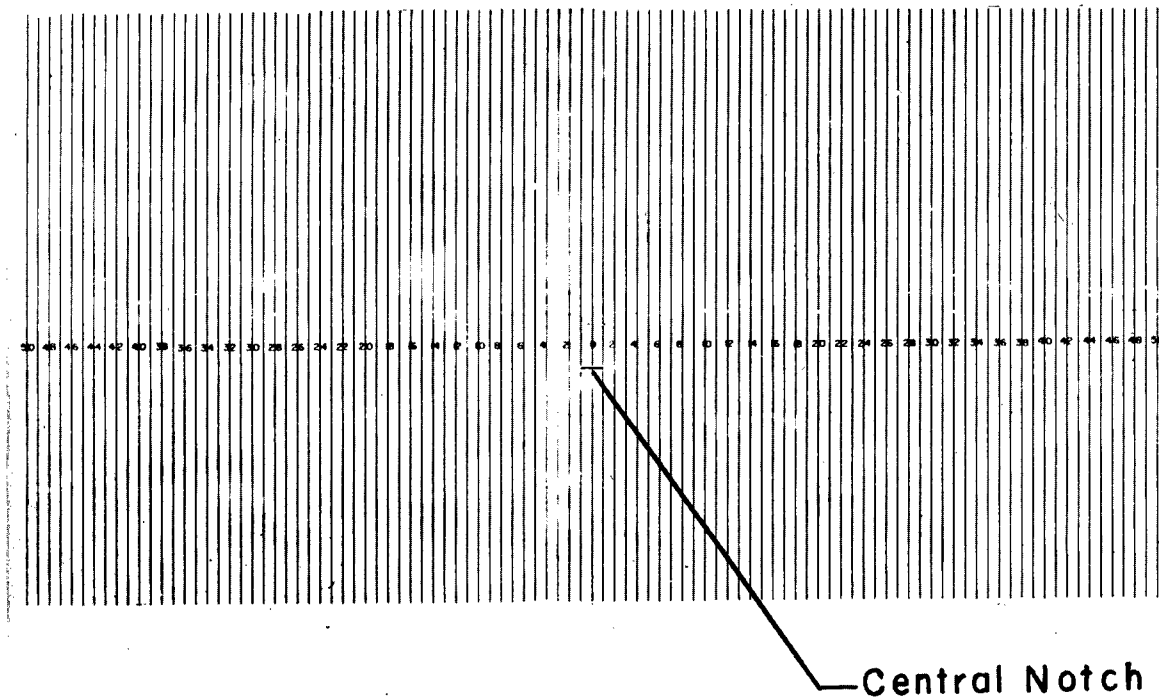
Figure 1.- Specimen configuration.

provide chemically clean specimen surfaces. Following cleaning the specimen blanks were heat treated according to the specifications outlined by the producer. After heat treatment a 1/10-inch-long (0.254-cm) central notch was cut into the center of each specimen by using an electrical discharge technique. The width

Rigid quality-control specifications were followed in the fabrication of all specimens. The sheet materials were covered with protective tape prior to shearing to insure unmarred specimen surfaces. Specimen blanks were carefully sheared and then stenciled for identification. For specimens not requiring heat treatment, the central notches were cut and reference grids were printed on the specimen surfaces photographically. When heat treatment was required, the specimen blanks were cleaned according to the procedures outlined by the producer of the material or according to procedures developed at the NASA Langley Research Center if no producer's procedures were available. All the cleaning procedures were designed to have no deleterious effects upon the materials and to provide

of the central notch was 0.010 ± 0.002 inch (0.254 ± 0.051 mm). The heat generated in this cutting process is very localized; consequently, the cutting process was believed to have little effect upon the material surrounding the notch.

A reference grid (fig. 2) was photographically printed on the surface of the specimen to mark intervals in the path of the crack. This reference grid



L-63-4299.1

Figure 2.- Grid used to mark intervals in crack path. Grid spacing is 0.05 in. (1.27 mm).

afforded ready observation of the crack front and provided a crack-growth path free of mechanical defects which might affect normal crack propagation. Before adopting the photographic reference grid, it was determined by metallographic examinations and tensile tests on specimens bearing the grid that the grid had no detrimental effects upon the materials at 550° F (561° K).

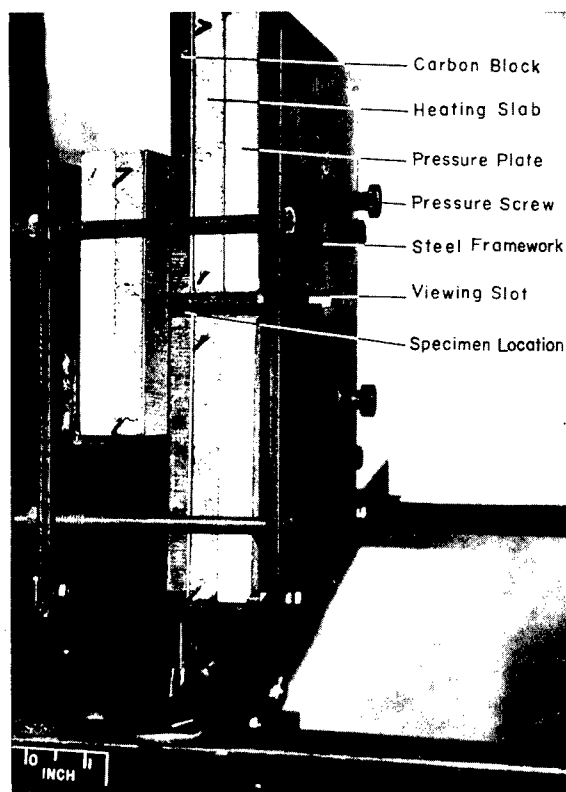
Testing Equipment

Axial-load fatigue-testing equipment used in this investigation included a subresonant machine, a hydraulic machine, and a combination hydraulic and subresonant machine. The subresonant machine had an operating frequency of 1800 cpm, a load capacity of $\pm 20,000$ pounds (± 89 kN), and cycle-counter reading in units of 100 cycles. The hydraulic machine had an operating frequency of

1200 cpm, a load capacity of 100,000 pounds (445 kN), and a cycle-counter reading in units of 100 cycles. As a hydraulic unit, the combination machine had an operating frequency of 50 cpm, a load capacity of 132,000 pounds (587 kN), and a cycle-counter reading in units of 1 cycle. As a subresonant unit this machine had an operating frequency of 820 cpm for the specimens used (a function of the natural frequency of the system), a load capacity of 110,000 pounds (489 kN), and a counter reading in units of 100 cycles. Each of these testing machines is further described in references 1, 2, and 3, respectively.

Loads were monitored continuously by measuring the output of a strain-gage bridge cemented to a weigh bar in series with the specimen. Monitoring precision was approximately ± 1 percent. Heat-deflecting baffles were used for thermal protection of the weigh bars on the 20,000-pound (89-kN) and the 100,000-pound (445-kN) testing machines. In the combination testing machine, no thermal protection was required for the weigh bars because of the horizontal arrangement of the bar with respect to the heating furnace.

Special apparatus was developed to conduct the elevated-temperature tests (fig. 3). Three 1/2-inch-thick (1.27-cm) graphite blocks were placed in contact with the specimens. Two were placed on the observation side, one above and the other below the region of crack growth. A 1/2-inch (1.27-cm) gap was used to provide an unobstructed view of the growing crack. The third block was located on the opposite surface of the specimen immediately adjacent to the crack-growth region. Adjacent to each graphite block was a ceramic heating slab and an insulating pressure plate, in that order. A steel framework having an observation cutout was used to hold the components in position during testing. The components were held against the specimen by three machine screws which jammed against the asbestos pressure plate. The screws were carefully tightened to insure thermal contact without introducing significant friction forces. The surfaces of each component were machine ground until 90-percent contact was obtained between the surfaces of adjacent components and between the graphite and the specimens.



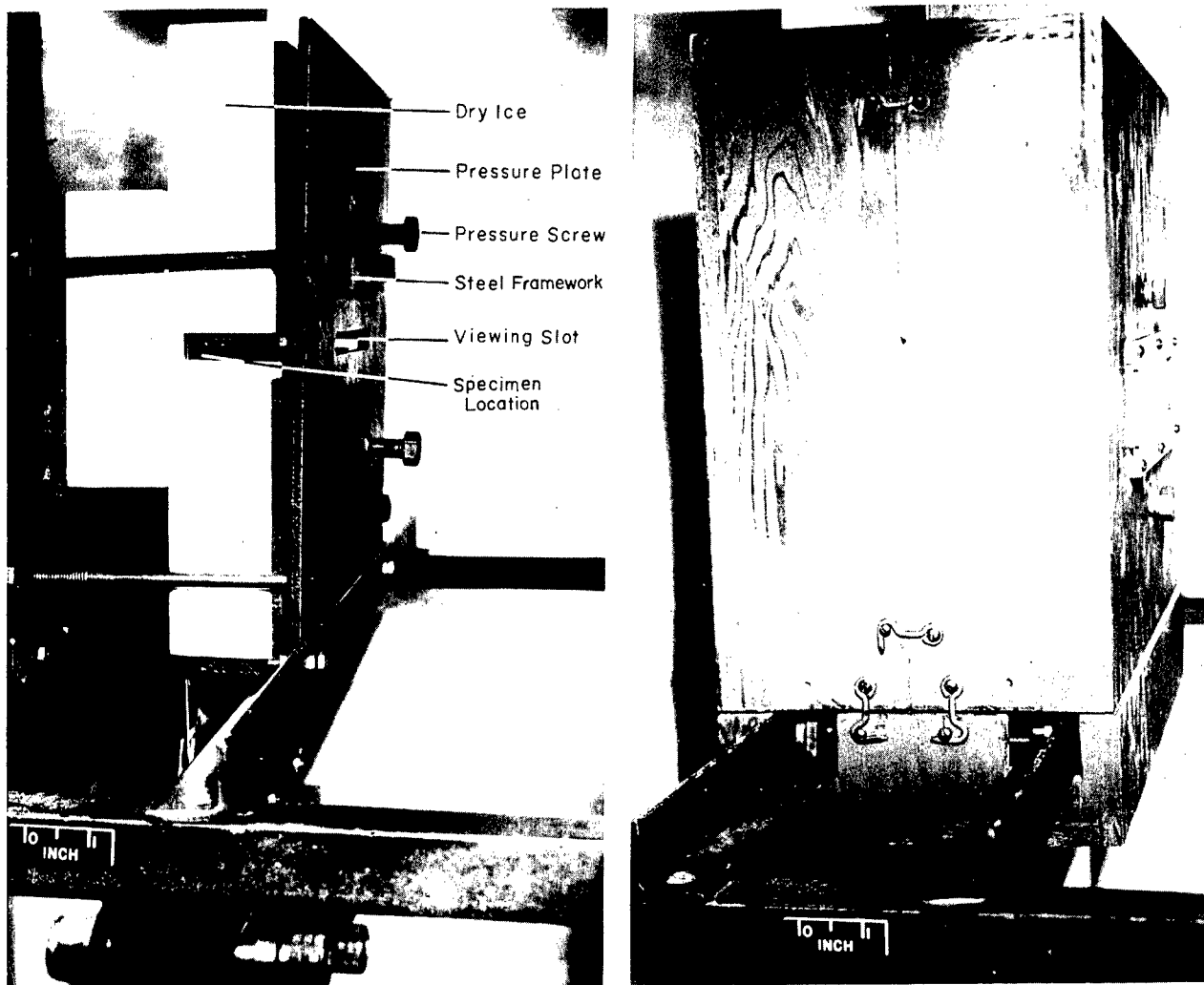
L-63-9528.1

Figure 3.- Elevated-temperature-test apparatus.

A chromel-alumel control thermocouple was spot welded in the projected crack path near the edge of the specimen. In preliminary tests, the temperature variation across the width of the specimen using an edge control point was found to be less than $\pm 5^{\circ}$ F ($\pm 3^{\circ}$ K).

Temperature control was maintained within $\pm 2^{\circ}$ F ($\pm 1^{\circ}$ K) in the 550° F (561° K) tests by a controller recorder which regulated current through a saturable reactor. The 60-cycle single-phase a-c controller operated on 208 volts.

The equipment used to conduct the cryogenic-temperature tests is shown in figure 4. Solid blocks of dry ice were mounted in the same steel framework used



(a) Steelwork with dry ice installed. L-63-9529.1

(b) Insulating box installed. L-63-9530

Figure 4.- Cryogenic-temperature-test apparatus.

for the furnace. These dry-ice blocks were held directly against the specimen surface in the same manner as the heating components. The temperature was controlled by the temperature of the dry ice and was found to vary less than $\pm 2^{\circ}$ F ($\pm 1^{\circ}$ K) across the width of the specimen. The average temperature was found to vary less than $\pm 5^{\circ}$ F ($\pm 3^{\circ}$ K) during the course of a test. The sublimation rate of the dry ice was satisfactorily controlled by insulating the entire cooling

apparatus from circulating air drafts. Frost buildup on the specimen surface was controlled by periodically spraying the specimen with ethyl alcohol.

In all the room-temperature tests and in the elevated- and cryogenic-temperature tests in which compressive loadings were applied, two lubricated guides similar to those described in reference 4 were used to prevent buckling and out-of-plane vibrations. Light oil was used to lubricate the surfaces of the specimen and of the guides in the room-temperature and cryogenic-temperature tests. In the elevated-temperature tests dry molybdenum disulfide was used for the lubricant. One of the two plates contained a 1/2-inch-wide (1.27-mm) cutout across the width of the plate to allow visual observation of the region of the crack. In the room- and cryogenic-temperature tests, a clear plexiglas insert was fitted into the cutout to prevent buckling in the observation region. In the elevated-temperature tests, a pyrex insert was used for this purpose.

Test Procedure

Constant-amplitude axial-load fatigue tests were conducted under positive mean stresses of 40 ksi (276 MN/m²) for the stainless steels and René 41 and 25 ksi (173 MN/m²) for the titanium alloys. All stresses mentioned herein refer to the initial net section of the specimens. Alternating stresses ranging from ±60 ksi (414 MN/m²) to ±5 ksi (30 MN/m²) for the stainless steels and René 41 and from ±25 ksi (173 MN/m²) to ±2 ksi (14 MN/m²) for the titanium alloys were applied to propagate the fatigue cracks. The mean and alternating loads were kept constant throughout each test.

Tests were conducted at room temperature and at elevated temperature on all materials with additional tests run at cryogenic temperature when sufficient material was available. Specimens were tested at the same stress levels at each of the temperatures in order to evaluate the effects of temperature on fatigue-crack growth.

In order to follow crack growth, fatigue cracks were observed through 30-power microscopes while illuminated by stroboscopic light. The number of cycles required to propagate the crack to each grid line was recorded and the tests were terminated when the cracks reached a predetermined crack length. Specimens tested in this investigation were reserved for a subsequent residual static-strength investigation (ref. 5).

RESULTS AND DISCUSSION

The results of fatigue-crack-propagation tests conducted on nine high-strength alloys are presented in table IV, which gives the average number of cycles required to grow the crack from a length x of 0.15 inch (0.381 cm) to the specified lengths. It was believed that at a crack length of 0.15 inch (0.381 cm), the crack propagation would no longer be affected by the notch used to initiate the crack. The quantity "number of cycles" given in the table and in figures 5 to 13 is the mean of the number of cycles required to produce cracks of equal length on both sides of the central notch.

Effect of Temperature

The fatigue-crack-propagation curves resulting from tests conducted at room temperature are compared with the curves from tests at elevated temperature and, when available, at cryogenic temperature in order to determine the effect of temperature upon the crack-propagation characteristics of each material. This comparison was made at each stress level by plotting on the same figure the variation of crack length with number of cycles for the room-, elevated-, and cryogenic-temperature tests. The differences between curves is a measure of the effect of temperature on fatigue-crack growth. The crack-growth resistance of the titanium alloys was essentially unchanged over the temperature range of the investigation, while the resistance of stainless steels and René 41 was slightly lower at elevated temperature than at room temperature.

The crack-propagation curves for AISI 301 and AM 350 (20-percent CRT) in figures 5 and 6 indicate that, for S_a of 20 ksi (138 MN/m^2) and higher, the cracks grew much faster at elevated temperature than at room temperature. For S_a of 10 ksi (68 MN/m^2) and 5 ksi (34 MN/m^2) cracks in these two materials grew slightly faster at room temperature than at elevated temperature. No explanation for this small reversal in resistance to crack growth can currently be offered. The decreased resistance at elevated temperature at the higher stress levels may be attributed to the deterioration of tensile properties at that temperature.

The crack-propagation curves for AM 350 (DA), PH 15-7Mo, PH 14-8Mo, and René 41 (figs. 7, 8, 9, and 10, respectively) show that cracks consistently propagated more rapidly at elevated temperature than at room temperature. The differences between curves for the AM 350 (DA) are greater at the higher stress levels which is consistent with the trend found in tests conducted on AISI 301 and AM 350 (20-percent CRT). The differences between the room-temperature and elevated-temperature fatigue-crack-growth curves are relatively small for PH 14-8Mo, PH 15-7Mo, and René 41. Fatigue-crack growth in PH 14-8Mo is generally slower at cryogenic temperature than at room temperature, but again the differences between curves are quite small.

The crack-growth characteristics of Ti-8Al-1Mo-1V (fig. 11) do not change appreciably over the temperature range -109° F (195° K) to 550° F (561° K). The crack-growth curves for Ti-6Al-4V (Annealed) and Ti-4Al-3Mo-1V (Aged) (figs. 12 and 13, respectively) show that these materials appeared slightly more resistant to crack growth at elevated temperature than at room temperature.

Ranking of Materials

Rates of crack propagation were obtained graphically by measuring the slopes of the crack-propagation curves at various crack lengths. Plots of fatigue-crack-propagation rate as a function of the ratio of alternating stress to mean stress, or load factor, are presented in figures 14, 15, and 16 for the room-, elevated-, and cryogenic-temperature tests. These plots were made for a crack length of 0.40 inch (1.02 cm). Similar plots (not presented) at both shorter and longer crack lengths indicate that the materials consistently

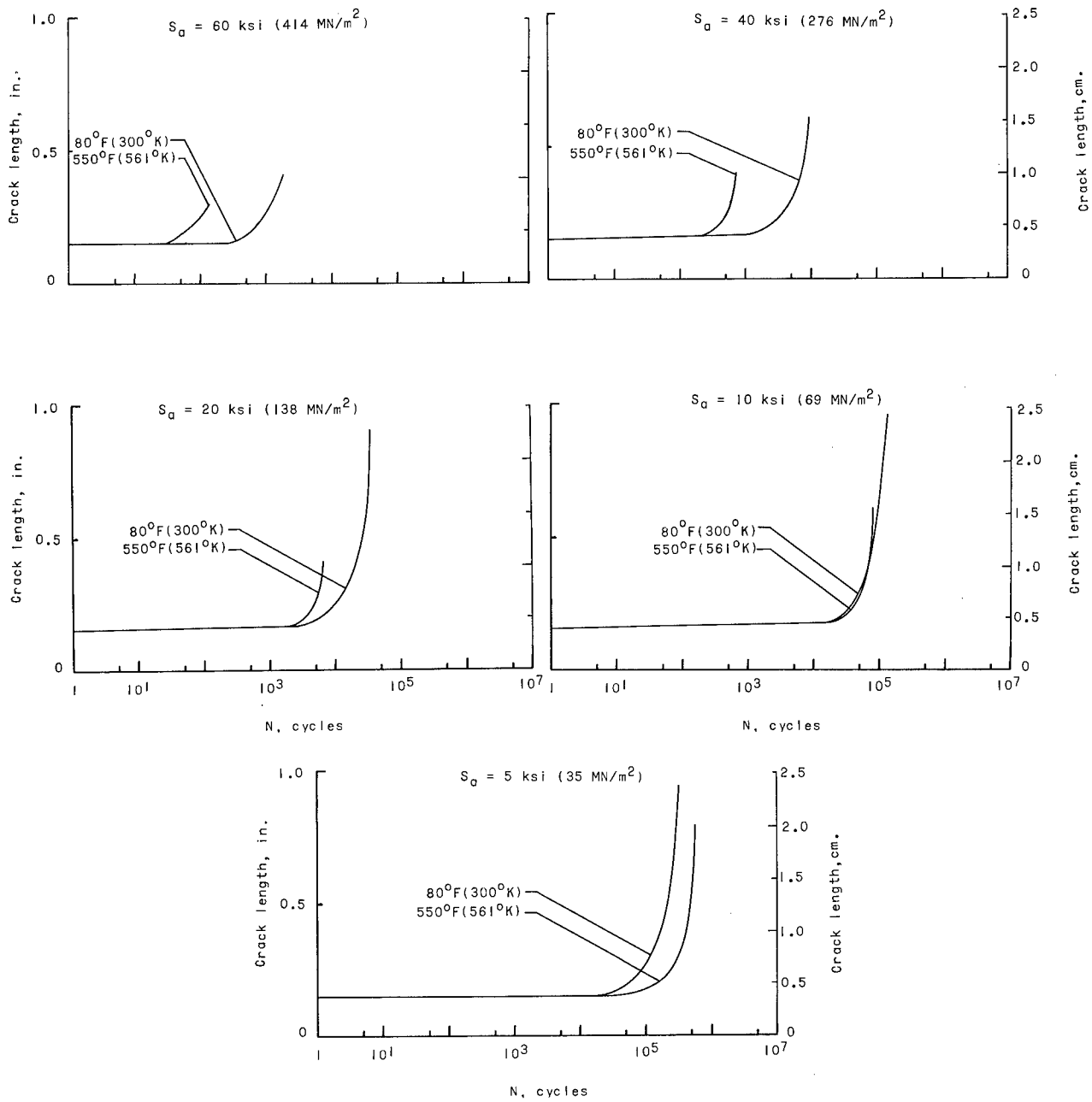


Figure 5.- Fatigue crack-propagation curves for AISI 301 (50-percent CR). $S_m = 40 \text{ ksi (276 MN/m}^2\text{)}$.

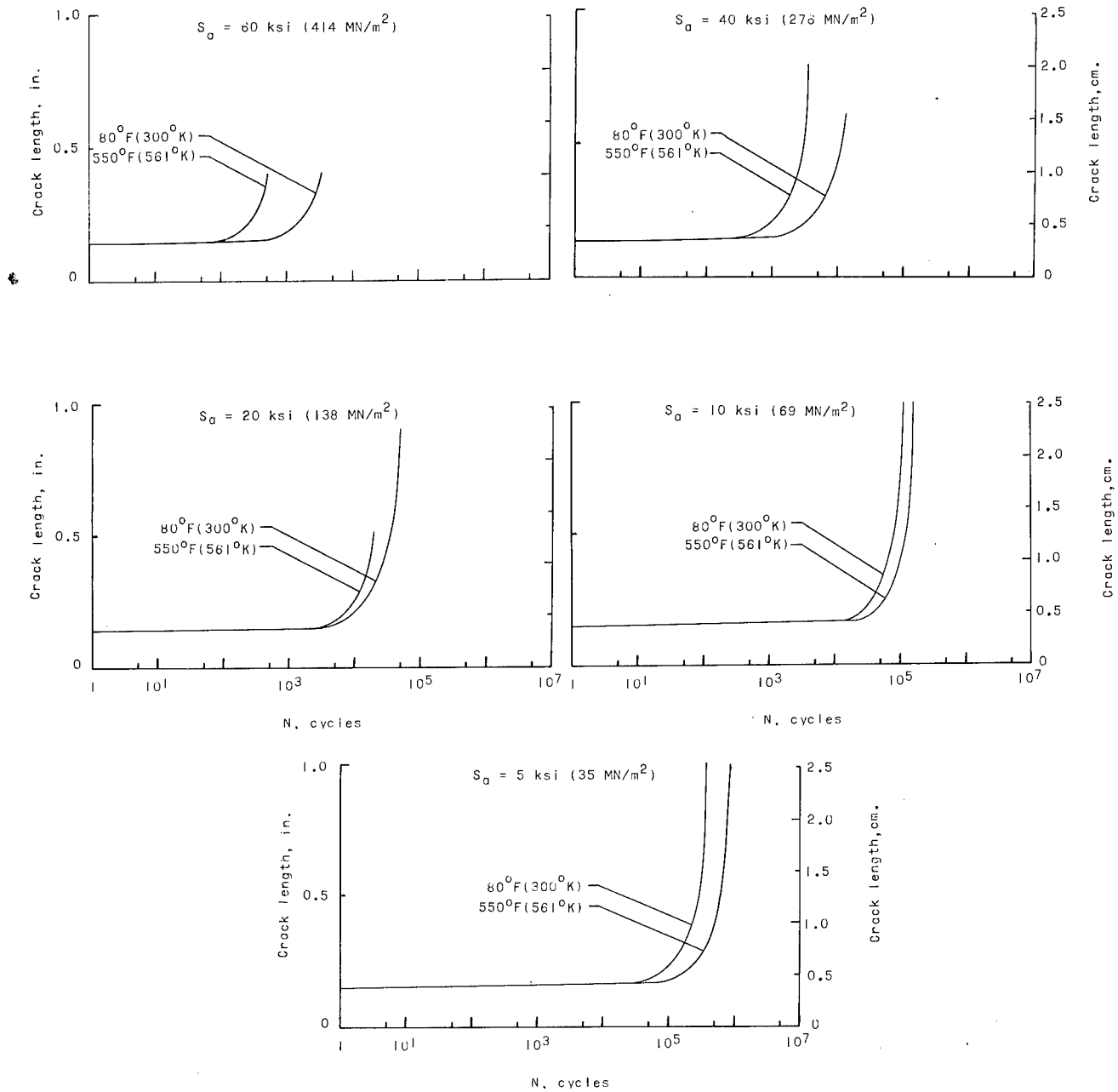


Figure 6.- Fatigue crack-propagation curves for AM 350 (20-percent CRT). $S_m = 40 \text{ ksi (276 MN/m}^2\text{)}$.

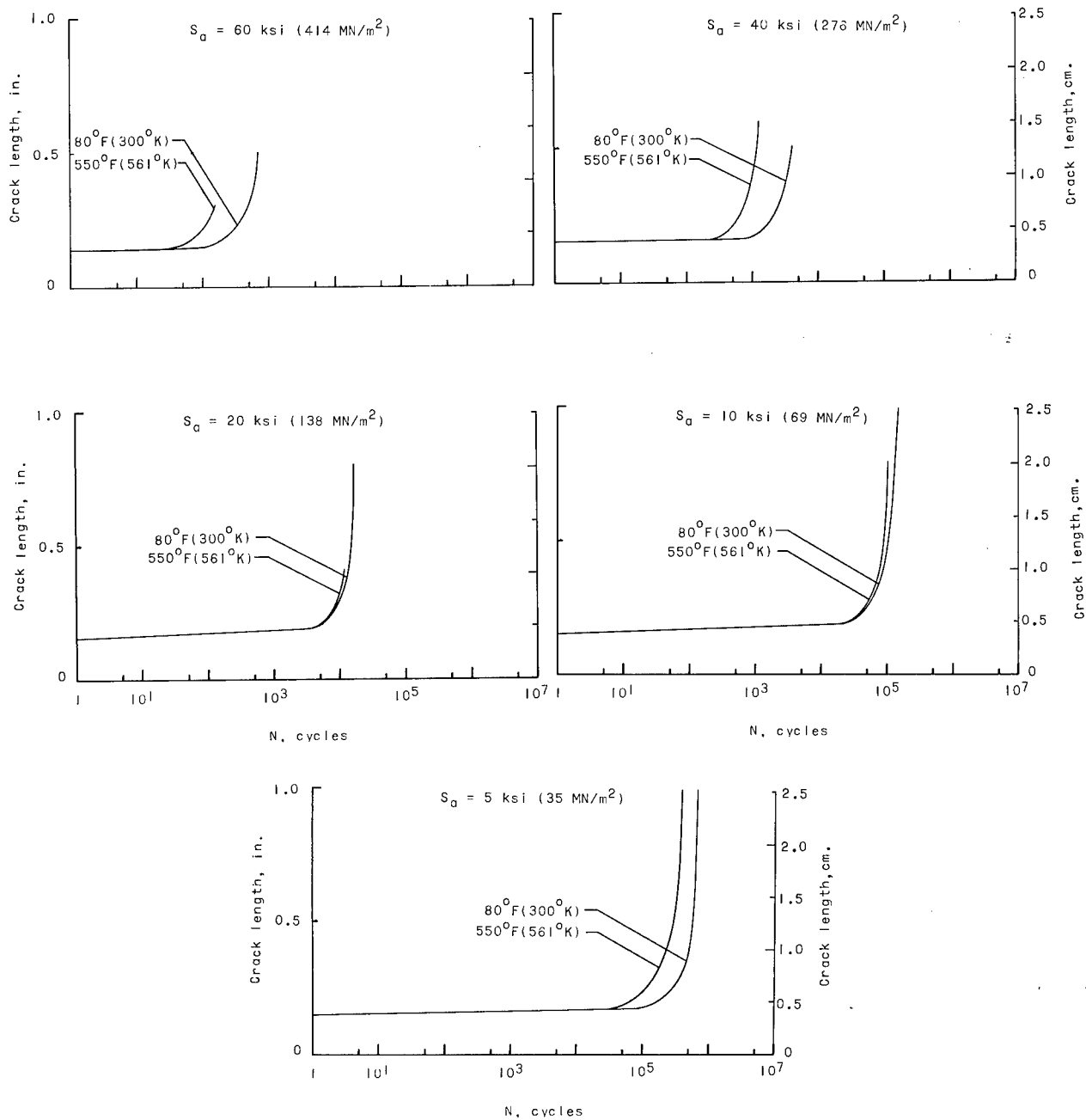


Figure 7.- Fatigue crack-propagation curves for AM 350 (DA). $S_m = 40 \text{ ksi (276 MN/m}^2\text{)}$.

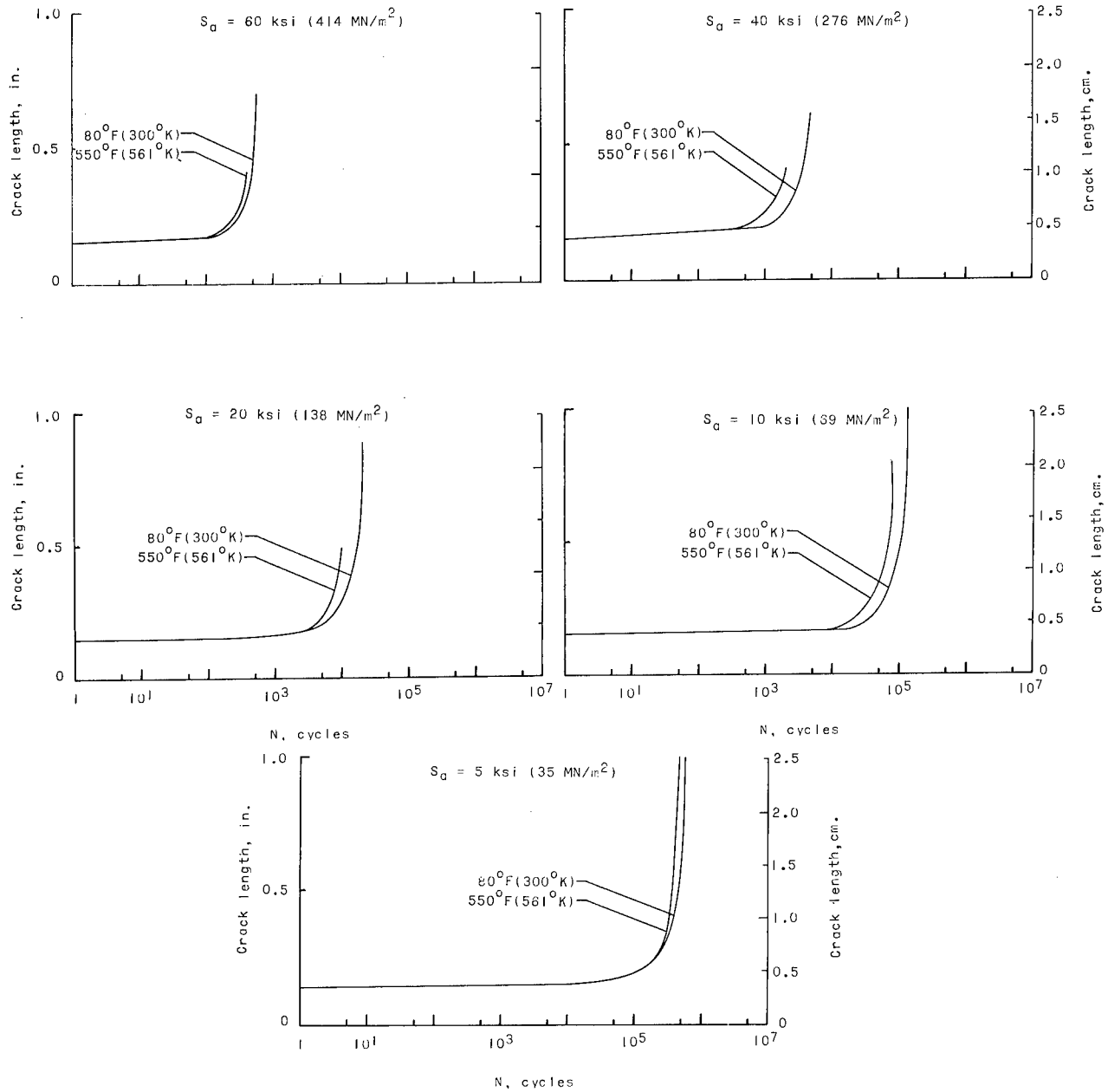


Figure 8.- Fatigue crack-propagation curves for PH 15-7Mo (TH 1050). S_m = 40 ksi (276 MN/m²).

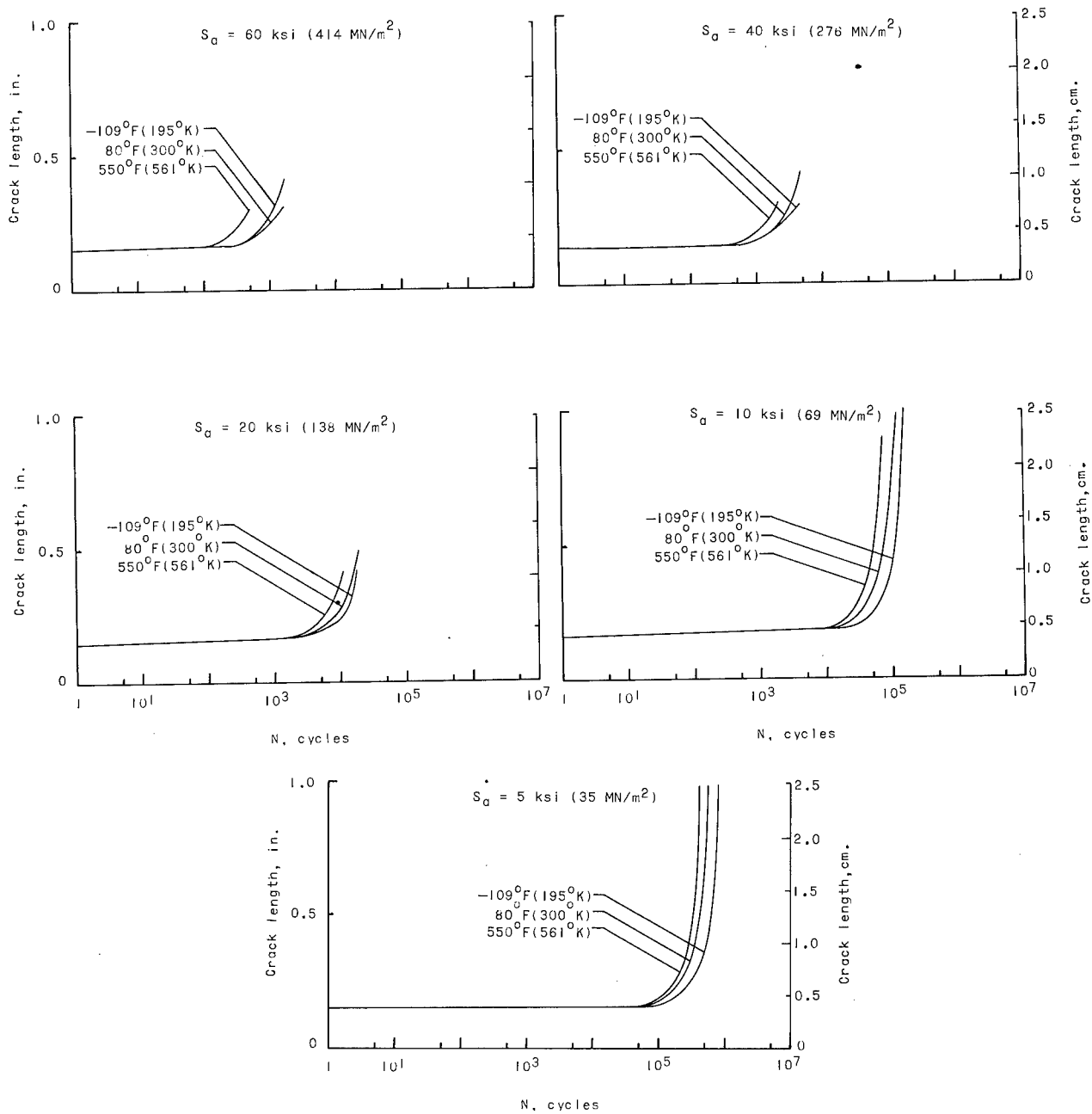


Figure 9.- Fatigue crack-propagation curves for PH 14-8Mo (SRH 950). $S_m = 40 \text{ ksi (276 MN/m}^2\text{)}$.

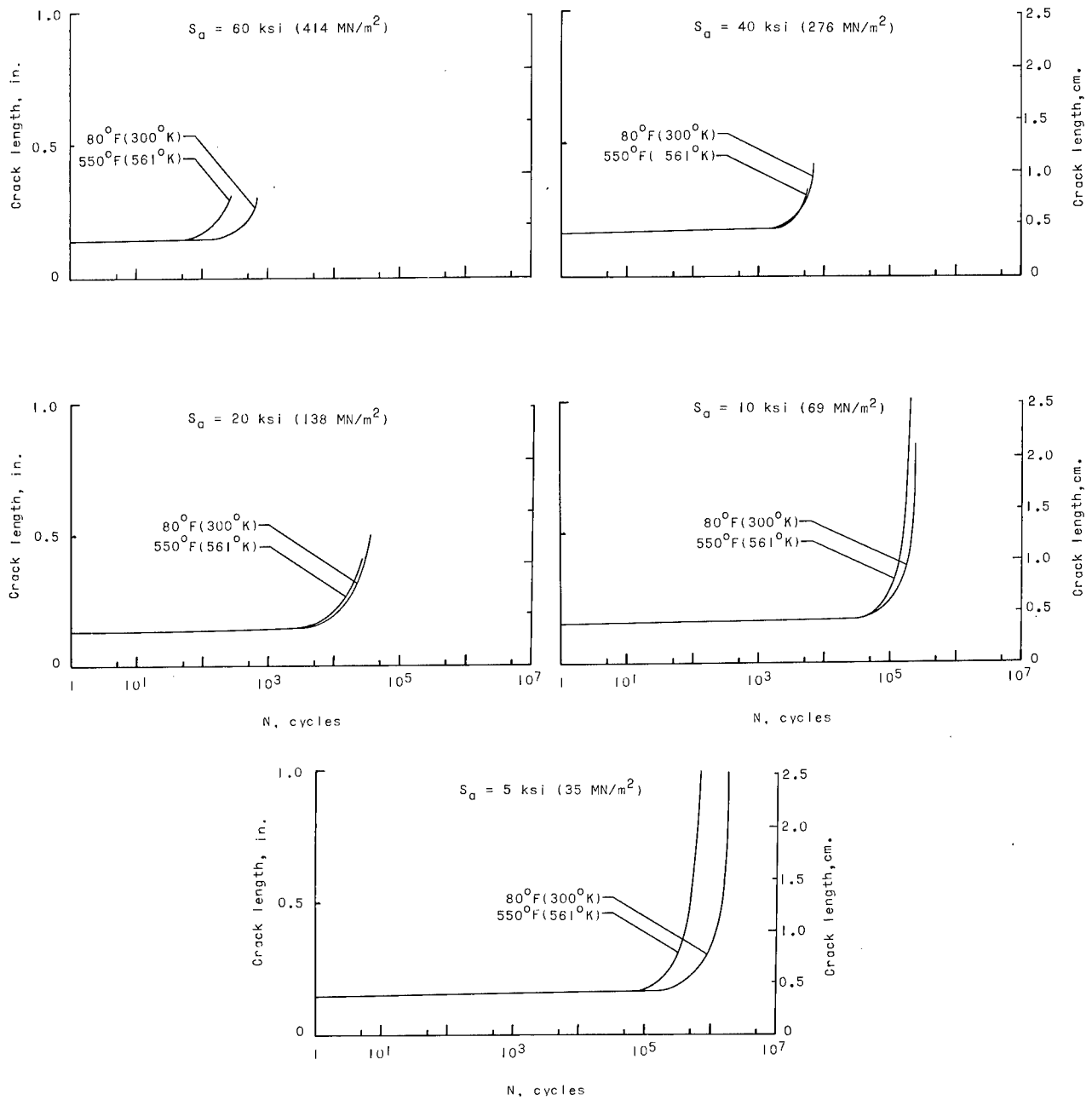


Figure 10.- Fatigue crack-propagation curves for René 41 (Condition B). $S_m = 40 \text{ ksi}$ (276 MN/m^2).

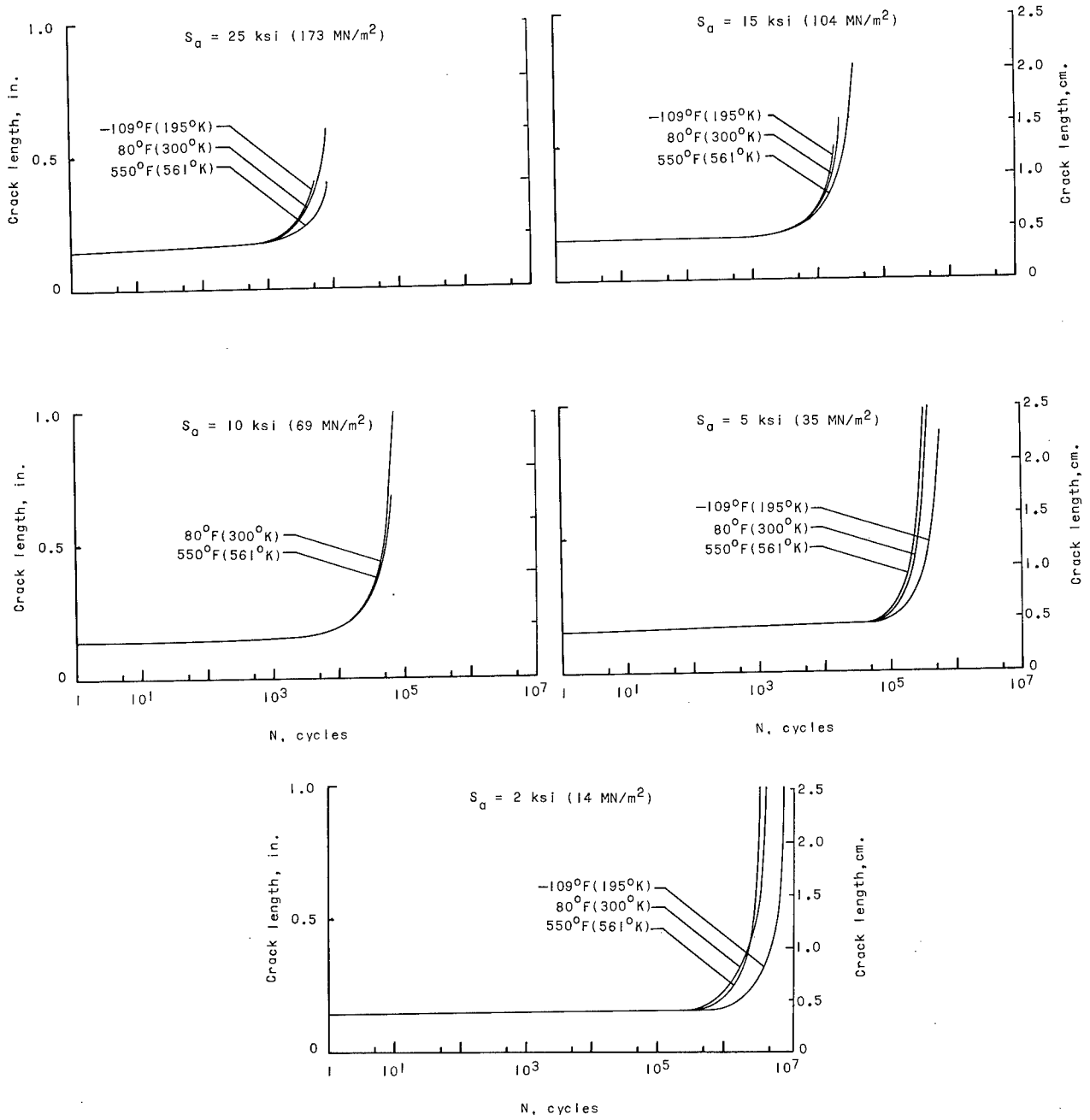


Figure 11.- Fatigue crack-propagation curves for Ti-8Al-1Mo-1V (Triplex Annealed).
 $S_m = 25 \text{ ksi}$ (173 MN/m^2).

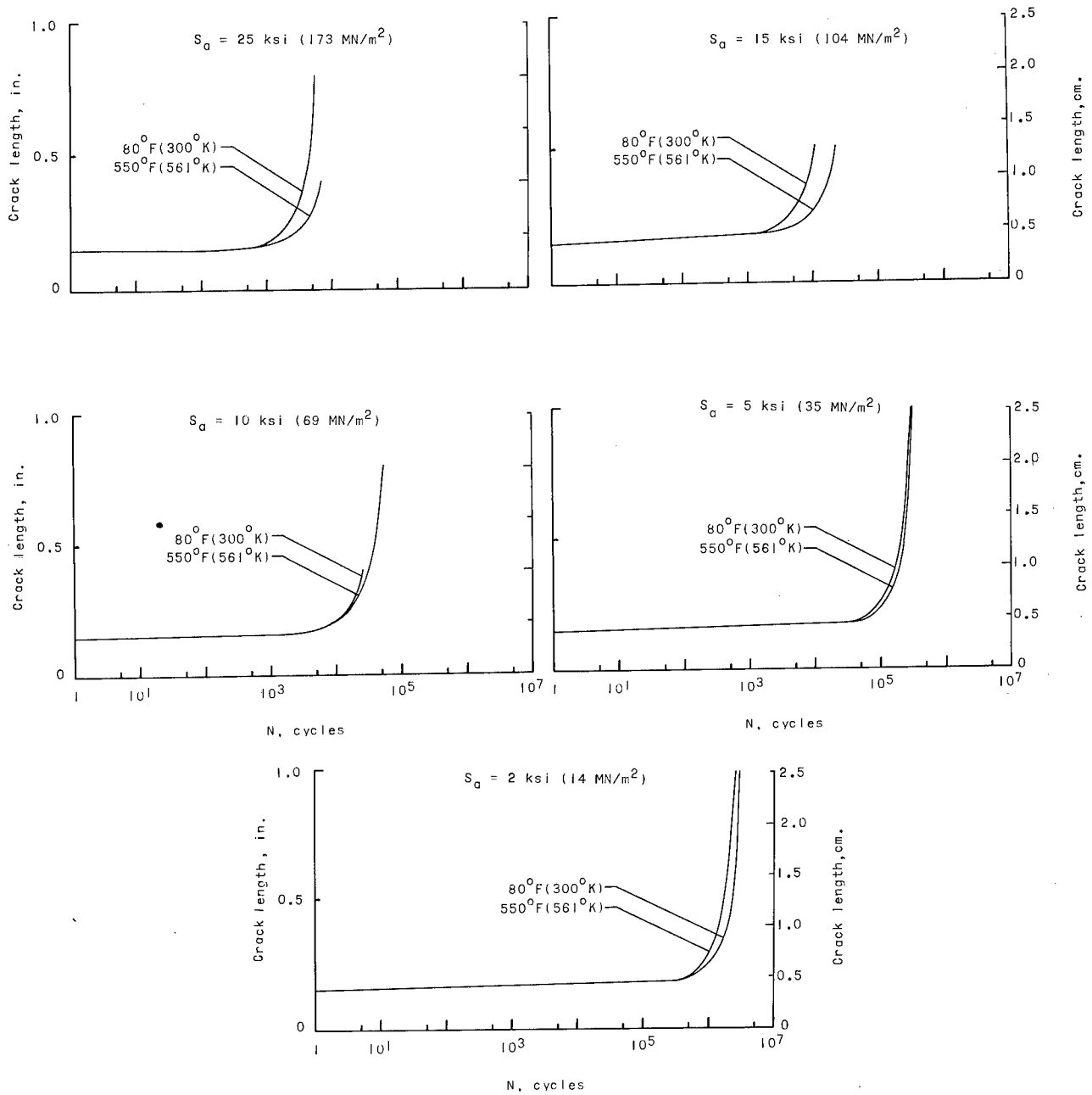


Figure 12.- Fatigue crack-propagation curves for Ti-6Al-4V (Annealed). S_m = 25 ksi (173 MN/m²).

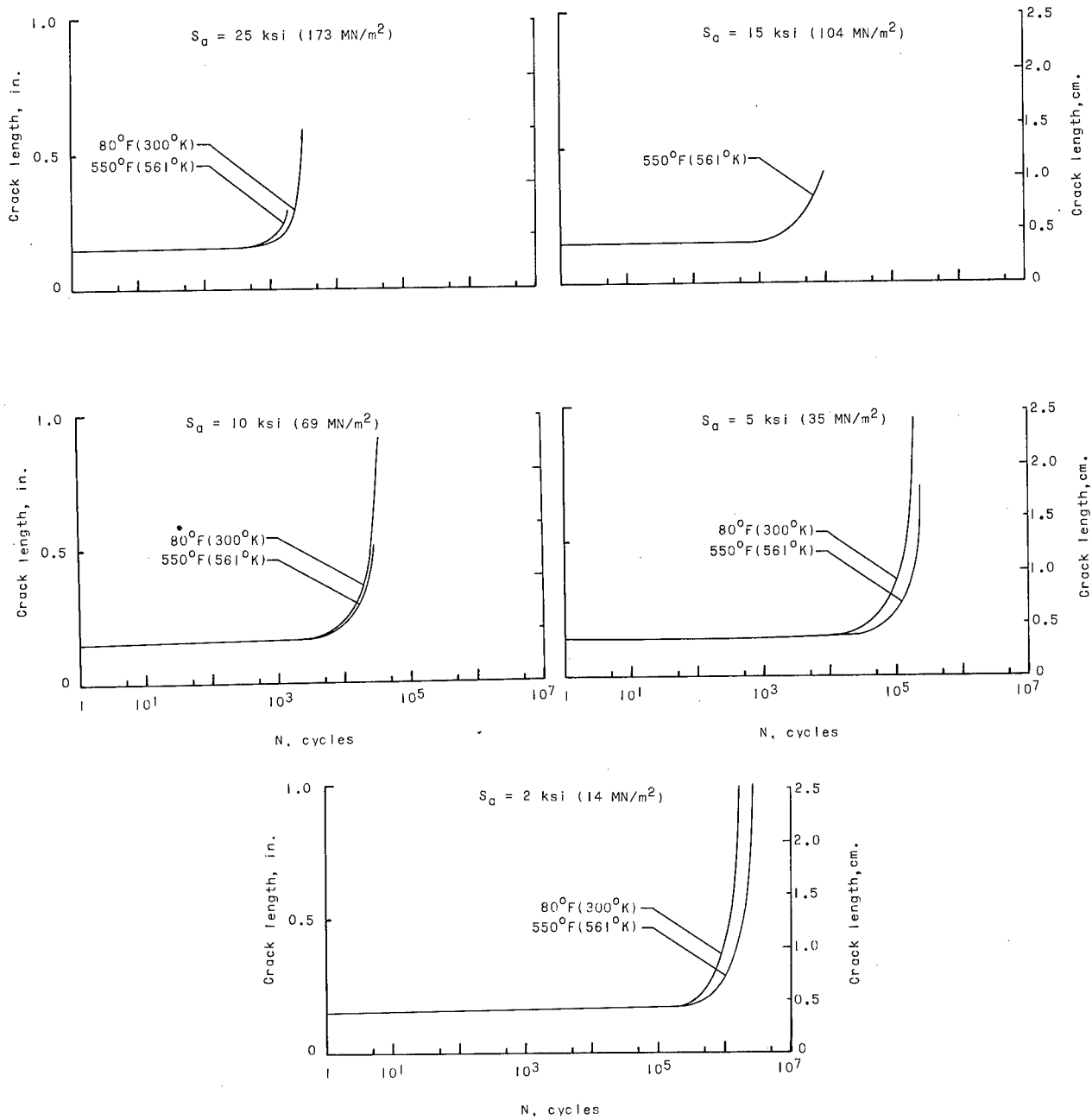


Figure 13.- Fatigue crack-propagation curves for Ti-4Al-3Mo-1V (Aged). $S_m = 25 \text{ ksi (173 MN/m}^2\text{)}$.

maintain the same relative positions. The results of tests on the stainless steels in which S_a was 60 ksi (414 MN/m^2) were omitted since there was no basis for comparison with the titanium alloys. In figures 14, 15, and 16 the lower the rate of crack propagation for a given load factor, the more resistant the material is to fatigue-crack growth. At room temperature (fig. 14) the titanium alloys, Ti-8Al-1Mo-1V and Ti-6Al-4V, and the René 41 appear to be the most resistant to crack propagation for load factors ranging from 0.13 to approximately 0.40. For higher load factors, 0.50 to 1.00, the AM 350 (20-percent CRT) stainless steel and the René 41 appear the most resistant to crack growth followed by Ti-8Al-1Mo-1V and AISI 301.

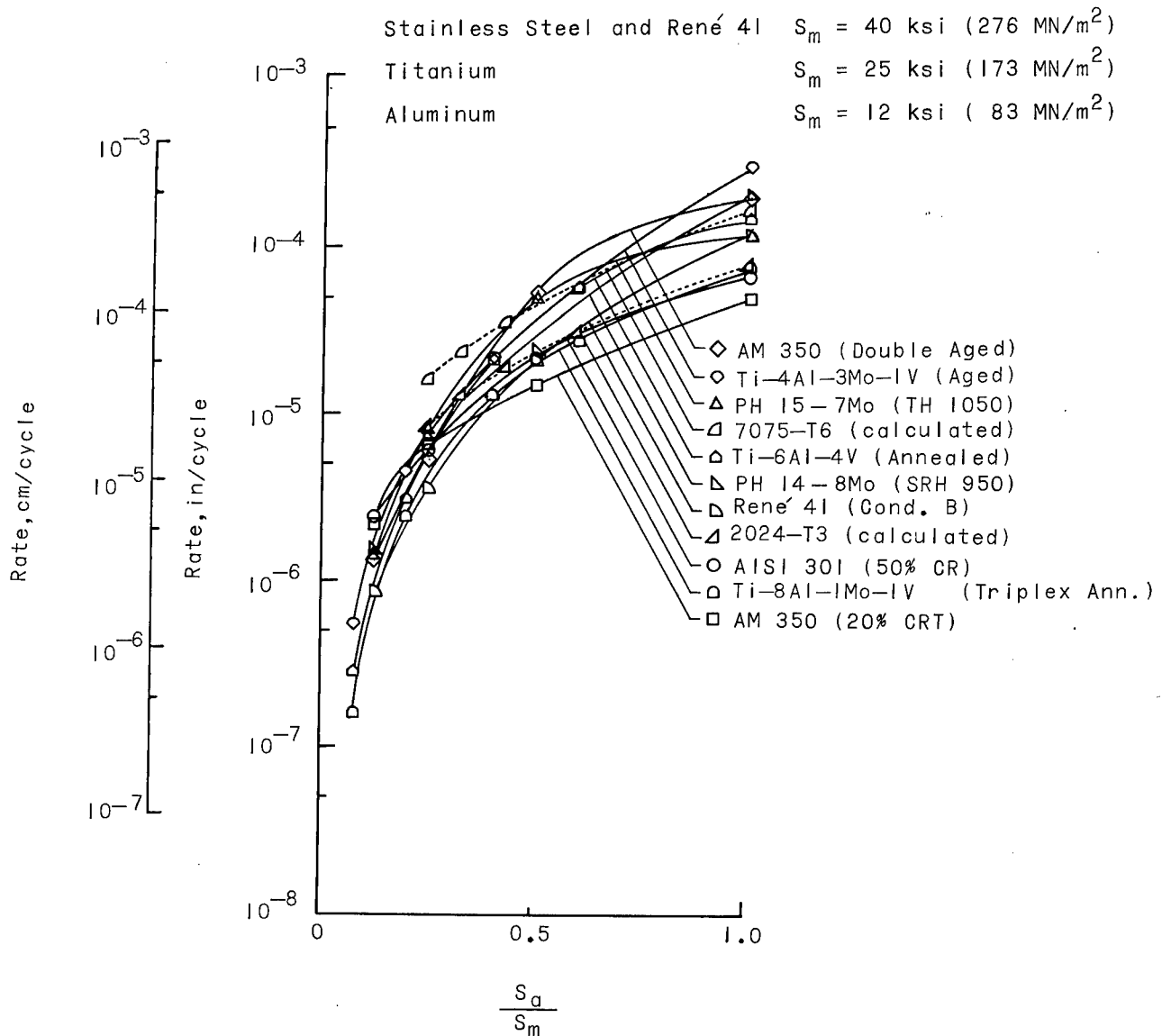


Figure 14.- Fatigue crack-propagation rate as a function of the ratio of alternating to mean stress at $80^\circ \text{ F } (300^\circ \text{ K})$ for a crack length x of 0.4 inch (1.02 cm).

Stainless Steel and René 41 $S_m = 40$ ksi (276 MN/m²)
 Titanium $S_m = 25$ ksi (173 MN/m²)

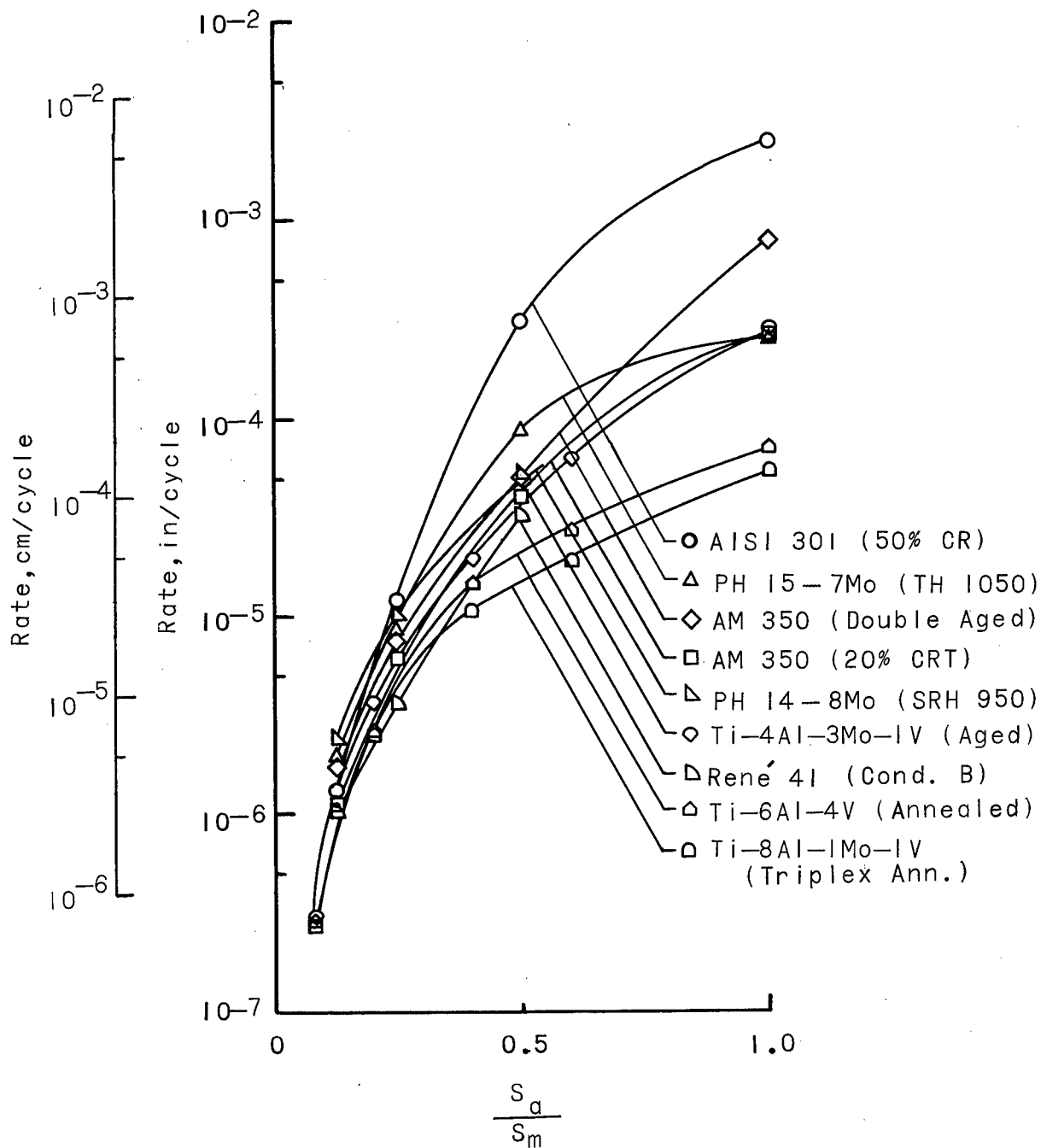


Figure 15.- Fatigue crack-propagation rate as a function of the ratio of alternating to mean stress at 550° F (561° K) for a crack length x of 0.4 inch (1.02 cm).

Stainless Steel and René 41 $S_m = 40$ ksi (276 MN/m²)

Titanium $S_m = 25$ ksi (173 MN/m²)

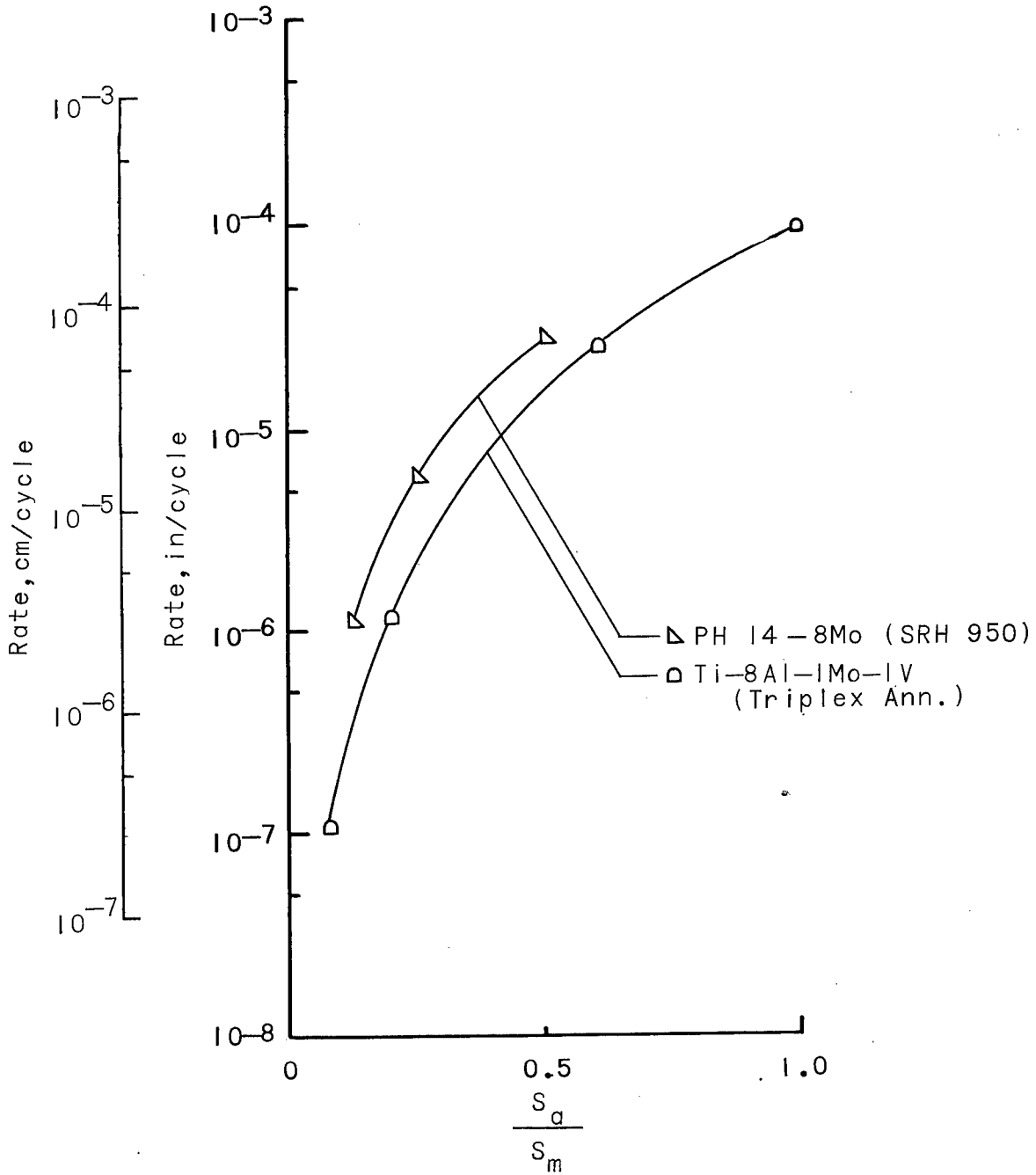


Figure 16.- Fatigue crack-propagation rate as a function of the ratio of alternating to mean stress at -109° F (195° K) for a crack length x of 0.4 inch (1.02 cm).

For purposes of comparison, calculated crack-growth rates (dashed curves) for 2024-T3 and 7075-T6 aluminum alloys were included in figure 14.^a A mean stress of 12 ksi (83 MN/m²) was assumed for these calculations. Inspection of figure 14 indicates that cracks grow at approximately the same rates in the 2024-T3 alloy as in the more resistant high-strength alloys, while crack-growth rates in the 7075-T6 alloy were similar to those in the least resistant high-strength alloys. The mean stresses at which the comparisons in figures 14 to 16 were made (i.e., 12 ksi (83 MN/m²) for aluminum, 25 ksi (173 MN/m²) for titanium alloys, and 40 ksi (276 MN/m²) for the stainless steels and René 41) are approximately equal to one-fifth of the ultimate tensile strength of the materials. By coincidence the mean stress-density ratios for the materials were also approximately equal. Thus, from the standpoint of fatigue-crack growth, the better high-strength alloys are at least as efficient as the conventionally used aluminum alloys.

At elevated temperature (fig. 15) Ti-8Al-1Mo-1V was most resistant to crack propagation over the entire range of load factors, followed by Ti-6Al-4V and René 41. At cryogenic temperature (fig. 16) Ti-8Al-1Mo-1V was most resistant to crack propagation over the entire range of load factors. Due to limited quantities of the other alloys, only Ti-8Al-1Mo-1V and PH 14-8Mo were tested at cryogenic temperature. From these comparisons, it appears that Ti-8Al-1Mo-1V exhibited the greatest resistance to fatigue-crack growth for temperatures ranging from -109° F (195° K) to 550° F (561° K). The superalloy René 41 appears to be the second most resistant material at both room and elevated temperatures.

CONCLUDING REMARKS

Results of fatigue-crack-propagation investigations at 550° F (561° K), 80° F (300° K), and, in some cases, -109° F (195° K) on sheet specimens made from nine high-strength alloys support the following general conclusions:

1. Overall, the titanium alloy Ti-8Al-1Mo-1V (Triplex Annealed) exhibited the greatest resistance to crack propagation for the temperature range /

^aCrack-growth rates for the aluminum alloys were calculated by using an empirical expression developed in reference 2. The rate of crack propagation is expressed as a function of the fatigue limit and the product of the net section stress and the theoretical stress-concentration factor modified for size effect. Fatigue limits for unnotched sheet specimens of 2024-T3 and 7075-T6 at the appropriate R values were obtained from reference 1. The theoretical stress-concentration factors were calculated by using the method outlined in reference 2. In a subsequent investigation (ref. 6) it was found that for different R values (i.e., 0 and -1), there was a small change in the constants in their fatigue-crack-rate expression. However, since this change in constants was relatively small, the constants developed in reference 2 were adopted for calculating the rates shown in figure 14.

-109° F (195° K) to 550° F (561° K). René 41 (Condition B) appeared to be the second most resistant material.

2. From the standpoint of fatigue-crack propagation, the high-strength alloys investigated exhibited approximately the same material efficiency as conventionally used aluminum alloys.

3. All five stainless-steel alloys and the René 41 exhibited greater resistance to crack growth at room temperature than at elevated temperature at the higher stress levels. This resistance was attributed to the normal deterioration of tensile properties at elevated temperature. At the two lowest stress levels, fatigue cracks in AM 350 (20-percent CRT) and AISI 301 (50-percent CR) were found to propagate slightly faster at room temperature than at elevated temperature.

4. The Ti-8Al-1Mo-1V exhibited essentially the same resistance to crack growth at elevated temperature as at room temperature while Ti-6Al-4V (Annealed) and Ti-4Al-3Mo-1V (Aged) were found to be slightly more resistant to crack growth at elevated temperature than at room temperature.

5. Of the stainless steels studied, AM 350 (20-percent CRT) exhibited the greatest resistance to crack propagation. At the higher stress levels, in the room-temperature tests this stainless steel exhibited the lowest rate of crack propagation of all materials tested. /

Langley Research Center,
National Aeronautics and Space Administration,
Langley Station, Hampton, Va., April 16, 1964.

APPENDIX

CONVERSION OF U.S. CUSTOMARY UNITS TO THE
INTERNATIONAL SYSTEM OF UNITS

The conversion factors used in converting from the U.S. Customary Units to the International System (SI) are listed herein.

To convert from U.S. Units	Multiply by -	To obtain International Units
lb	4.448222	newton (N)
in.	2.54×10^{-2}	meters (m)
ksi	6.894757	meganewton/meter ² (MN/m ²)
°F	$5/9(^{\circ}\text{F} + 459.67)$	degrees Kelvin (°K)

Prefixes and symbols to indicate multiples of units are as follows:

Multiple	Prefix	Symbol
10^{-3}	milli	m
10^{-2}	centi	c
10^3	kilo	k
10^6	mega	M
10^9	giga	G

REFERENCES

1. Grover, H. J., Hyler, W. S., Kuhn, Paul, Landers, Charles B., and Howell, F. M.: Axial-Load Fatigue Properties of 24S-T and 75S-T Aluminum Alloy as Determined in Several Laboratories. NACA Rep. 1190, 1954. (Supersedes NACA TN 2928.)
2. McEvily, Arthur J., Jr., and Illg, Walter: The Rate of Fatigue-Crack Propagation in Two Aluminum Alloys. NACA TN 4394, 1958.
3. Hudson, C. Michael, and Hardrath, Herbert F.: Investigation of the Effects of Variable-Amplitude Loadings on Fatigue Crack Propagation Patterns. NASA TN D-1803, 1963.
4. Brueggeman, W. C., and Mayer, M., Jr.: Guides for Preventing Buckling in Axial Fatigue Tests of Thin Sheet-Metal Specimens. NACA TN 931, 1944.
5. Figge, I. E.: Residual Static Strength of Several Titanium and Stainless-Steel Alloys and One Superalloy at -109° F, 70° F, and 550° F. NASA TN D-2045, 1963.
6. Illg, Walter, and McEvily, Arthur J., Jr.: The Rate of Fatigue-Crack Propagation for Two Aluminum Alloys Under Completely Reversed Loading. NASA TN D-52, 1959.

TABLE I.- MATERIAL HEAT TREATMENTS

Material	Condition	Heat treatment
Ti-4Al-3Mo-1V	Aged	1650° F (1172° K) for 20 minutes; water quenched; 1050° F (839° K) for 4 hours; air cooled
Ti-6Al-4V	Annealed (mill)	1475° F (1075° K) for 1 hour; furnace cooled to 1300° F (978° K); air cooled
Ti-8Al-1Mo-1V	Triplex annealed	1450° F (1061° K) for 8 hours; furnace cooled; 1850° F (1283° K) for 5 minutes; air cooled; 1375° F (1019° K) for 15 minutes; air cooled
AM 350	Double aged	Received in Condition H; 1375° F (1019° K) for 3 hours; air cooled to 80° F (300° K) maximum; 850° F (728° K) for 3 hours; air cooled
AM 350	20-percent CRT	20-percent cold rolled; aged in hot caustic at 930° F (772° K) for 3 to 5 minutes
AISI 301	50-percent CR	52-percent cold rolled
PH 15-7Mo	TH 1050	1400° F (1033° K) for 90 minutes; cooled to 60° F (289° K) within 1 hour; hold 30 minutes; heat to 1050° F (839° K) for 90 minutes; air cooled
PH 14-8Mo	SRH 950	1700° F ± 15° F (1101° K ± 8° K) for 60 minutes; air cooled; -100° F ± 10° F (200° K ± 6° K) for 8 hours; 950° F ± 10° F (783° K ± 6° K) for 60 minutes; air cooled
René 41	Condition B	1950° F (1339° K) for 3 hours; air cooled; 1400° F (1033° K) for 16 hours; air cooled

Card 4/9

57442

Ti, SS, NiB

All
TABLE II.- AVERAGE TENSILE PROPERTIES OF MATERIALS STUDIED

Temperature		σ_u		σ_y		E		e, percent	Number of tests
$^{\circ}\text{F}$	$^{\circ}\text{K}$	ksi	MN/m ²	ksi	MN/m ²	ksi	GN/m ²		
Ti-4Al-3Mo-1V (Aged)									
-109	195	164.3	1132	143.2	987	16.0×10^3	110	12.5	5
70	294	139.1	958	120.0	827	15.5	107	10.7	5
550	561	102.0	703	88.0	606	14.6	101	7.3	3
Ti-6Al-4V (Annealed)									
-109	195	170.8	1177	163.0	1123	17.4×10^3	120	13.2	5
70	294	144.4	995	137.3	946	16.4	113	12.5	5
550	561	109.1	752	96.7	666	14.4	99	7.5	5
Ti-8Al-1Mo-1V (Triplex Annealed)									
-109	195	178.6	1231	161.8	1115	18.3×10^3	126	15.6	4
70	294	153.3	1056	140.0	965	18.2	125	13.6	5
550	561	120.0	827	98.0	675	16.0	110	11.0	3
AM 350 (Double Aged)									
-109	195	211.7	1459	178.0	1226	30.1×10^3	207	19.0	5
70	294	186.0	1282	154.9	1067	28.5	196	16.0	5
550	561	165.3	1139	124.0	854	27.8	191	7.1	3
AM 350 (20-percent CRT)									
-109	195	251.4	1732	175.2	1207	28.9×10^3	199	19.0	5
70	294	204.5	1409	182.3	1256	28.6	197	18.8	5
550	561	158.3	1091	154.7	1066	27.9	192	2.7	4
AISI 301 (50-percent CR)									
-109	195	234.8	1618	203.7	1403	29.5×10^3	203	29.0	5
70	294	212.0	1461	189.7	1307	25.6	176	5.0	5
550	561	178.6	1231	149.3	1029	23.2	160	2.6	3
PH 15-7Mo (TH 1050)									
-109	195	219.3	1511	209.5	1443	30.8×10^3	212	10.0	5
70	294	199.9	1377	195.0	1344	29.2	201	8.5	5
550	561	179.2	1235	177.3	1222	24.8	171	3.0	3
PH 14-8Mo (SRH 950)									
-109	195	272.8	1880	234.4	1615	29.4×10^3	203	13.4	5
70	294	243.3	1676	209.0	1440	28.7	198	8.7	3
550	561	202.3	1394	174.5	1202	23.3	161	8.5	3
René 41 (Condition B)									
-109	195	201.0	1385	143.2	987	31.0×10^3	214	17.8	3
70	294	189.8	1308	138.3	953	30.8	212	17.5	3
550	561	171.5	1182	133.4	919	30.3	209	9.5	3

Card 5/9

57442

Ti, SS, NiB

TABLE III.- NOMINAL CHEMICAL COMPOSITION OF MATERIALS

Material	C	Mn	P	S	Si	Cu	Ni	Cr	Mo	V	Al	N	H	Ti	Fe	O	B	Co
TI-4Al-3Mo-1V	0.08 max.								2.5 to 3.5	0.75 to 1.25	3.75 to 4.75	0.05 to max.	0.015 to max.	Bal- ance	0.25 max.			
TI-6Al-4V	0.10 max.									3.50 to 4.50	5.50 to 6.75	0.05 to max.	0.015 to max.	Bal- ance	0.30 max.	0.20 max.		
TI-8Al-1Mo-1V	0.08 max.								0.75 to 1.25	0.75 to 1.25	7.50 to 8.50	0.05 to max.	0.015 to max.	Bal- ance	0.30 max.			
AM 350	0.08 to 0.12	0.50 to 1.25	0.040 to max.	0.030 to max.	0.50 to max.		4.00 to 5.00	16.00 to 17.00	2.50 to 3.25			0.07 to 0.13			Bal- ance			
AISI 301	0.08 to 0.15	2.00 to max.	0.040 to max.	0.030 to max.	1.00 to max.	0.50 to max.	7.00 to 10.00	17.00 to 19.00	0.50 to max.						Bal- ance			
PH 15-7Mo	0.09 max.	1.00 max.	0.04 to max.	0.03 to max.	1.00 to max.		6.50 to 7.75	14.00 to 16.00	2.00 to 3.00		0.75 to 1.50				Bal- ance			
PH 14-8Mo	0.02 to 0.05	1.00 to max.	0.015 to max.	0.015 to max.	1.00 to max.		7.50 to 9.50	13.50 to 15.50	2.00 to 3.00		0.75 to 1.50				Bal- ance			
René 41	0.06 to 0.12	0.50 to max.			0.50 to max.		Bal- ance	18.00 to 20.00	9.00 to 10.50		1.50 to 1.80			3.00 to 3.30	5.00 to max.	0.010 to max.	10.00 to 12.00	

TABLE IV.- AVERAGE CRACK PROPAGATION CHARACTERISTICS OF MATERIALS TESTED

(a) AISI 301 (50-percent CR); $S_m = 40 \text{ ksi}$ (276 MN/m^2)

S_a		Number of cycles required to propagate crack from length of 0.15 inch (0.381 cm) to a length of:												
ksi	MN/m^2	0.20 in. (0.508 cm)	0.30 in. (0.762 cm)	0.40 in. (1.016 cm)	0.50 in. (1.270 cm)	0.60 in. (1.524 cm)	0.70 in. (1.778 cm)	0.80 in. (2.032 cm)	0.90 in. (2.286 cm)	1.00 in. (2.540 cm)	1.20 in. (3.048 cm)	1.40 in. (3.556 cm)	1.60 in. (4.064 cm)	1.80 in. (4.572 cm)
Temperature = 80° F (300° K)														
60	414	650	1,370	1,760										
40	276	2,250	5,375	7,260	8,525	9,340								
20	138	6,400	15,400	21,400	25,400	29,000	31,500	33,450	35,000					
10	69	19,000	46,000	65,500	78,000	92,500	102,000	109,500	115,000	120,000	127,500			
a5	35	55,000	121,000	172,000	208,000	238,000	260,000	278,000	293,000	305,000	324,000	337,000	344,000	347,000
Temperature = 550° F (561° K)														
60	414	60	165											
40	276	400	620	710										
20	138	3,800	5,800	6,300										
10	69	28,000	51,000	63,000	69,500	72,500								
a5	35	150,000	282,000	368,000	430,000	475,000	500,000	512,000						

(b) AM 350 (20-percent CRT); $S_m = 40 \text{ ksi}$ (276 MN/m^2)

S_a		Number of cycles required to propagate crack from length of 0.15 inch (0.381 cm) to a length of:												
ksi	MN/m^2	0.20 in. (0.508 cm)	0.30 in. (0.762 cm)	0.40 in. (1.016 cm)	0.50 in. (1.270 cm)	0.60 in. (1.524 cm)	0.70 in. (1.778 cm)	0.80 in. (2.032 cm)	0.90 in. (2.286 cm)	1.00 in. (2.540 cm)	1.20 in. (3.048 cm)	1.40 in. (3.556 cm)	1.60 in. (4.064 cm)	1.80 in. (4.572 cm)
Temperature = 80° F (300° K)														
60	414	1,240	2,680	3,430										
40	276	3,320	6,750	9,500	11,400	12,750								
20	138	9,000	19,800	27,300	33,800	39,000	42,200	46,200	49,300					
10	69	20,000	46,000	63,600	76,600	86,400	94,000	100,000	105,000	109,000	114,000	118,700		
a5	35	66,000	155,000	214,000	254,000	280,000	299,000	314,000	326,000	336,000	344,000			
Temperature = 550° F (561° K)														
60	414	225	417	515										
40	276	975	2,025	2,500	2,825	3,075	3,275	3,450						
20	138	5,300	12,300	16,200	18,400									
10	69	41,000	71,500	103,000	116,500	126,000	133,000	139,000	144,000	148,000	154,000			
a5	35	165,000	340,000	440,000	520,000	560,000	636,000	683,000	724,000	765,000	811,500	878,000		

(c) René 41 (Condition B); $S_m = 40 \text{ ksi}$ (276 MN/m^2)

S_a		Number of cycles required to propagate crack from length of 0.15 inch (0.381 cm) to a length of:												
ksi	MN/m^2	0.20 in. (0.508 cm)	0.30 in. (0.762 cm)	0.40 in. (1.016 cm)	0.50 in. (1.270 cm)	0.60 in. (1.524 cm)	0.70 in. (1.778 cm)	0.80 in. (2.032 cm)	0.90 in. (2.286 cm)	1.00 in. (2.540 cm)	1.20 in. (3.048 cm)	1.40 in. (3.556 cm)	1.60 in. (4.064 cm)	1.80 in. (4.572 cm)
Temperature = 80° F (300° K)														
60	414	430	700											
40	276	2,470	5,590	6,700										
20	138	10,400	21,300	27,500	32,000									
10	69	54,000	120,000	157,000	181,000	197,000	206,000	212,000	216,000					
a5	35	350,000	890,000	1,200,000	1,390,000	1,475,000	1,547,000	1,597,000	1,634,000	1,664,000	1,706,000	1,715,000		
Temperature = 550° F (561° K)														
60	414	167	280											
40	276	2,540	4,890											
20	138	8,700	19,300	24,000										
10	69	52,000	94,000	121,000	144,000	160,000	170,000	177,000	182,000	185,000				
a5	35	146,000	316,000	421,000	496,000	549,000	596,000	638,000	671,000	700,000	736,000	741,000	772,000	778,000

^aCrack initiated at S_a of 10 ksi (69 MN/m^2) to expedite testing.

Card 7/9

57442

Ti, SS, NiB

TABLE IV.- AVERAGE CRACK PROPAGATION CHARACTERISTICS OF MATERIALS TESTED - Continued

(d) AM 350 (Double Aged); $S_m = 40$ ksi (276 MN/m²)

S_a		Number of cycles required to propagate crack from length of 0.15 inch (0.381 cm) to a length of:												
ksi	MN/m ²	0.20 in. (0.508 cm)	0.30 in. (0.762 cm)	0.40 in. (1.016 cm)	0.50 in. (1.270 cm)	0.60 in. (1.524 cm)	0.70 in. (1.778 cm)	0.80 in. (2.032 cm)	0.90 in. (2.286 cm)	1.00 in. (2.540 cm)	1.20 in. (3.048 cm)	1.40 in. (3.556 cm)	1.60 in. (4.064 cm)	1.80 in. (4.572 cm)
Temperature = 80° F (300° K)														
60	414	260	510	626	693									
40	276	1,540	2,980	3,680	4,080									
20	138	4,950	10,150	12,700	14,320	15,570	16,500	17,260						
10	69	28,000	61,000	82,000	98,000	110,000	120,000	126,000	132,000	136,000	142,000			
a ₅	35	170,000	373,000	476,000	541,000	585,000	619,000	642,000	658,000	669,000	680,000	684,000		
Temperature = 550° F (561° K)														
60	414	90	160											
40	276	440	850	1,040	1,120	1,200								
20	138	4,100	9,600	12,400										
10	69	24,500	57,500	75,500	87,000	94,500	100,000	104,500						
a ₅	35	56,000	150,000	216,000	264,000	302,000	333,000	354,000	371,000	384,000	404,000	424,000	426,000	

(e) Ti-8Al-1Mo-1V (Triplex Annealed); $S_m = 25$ ksi (173 MN/m²)

S_a		Number of cycles required to propagate crack from length of 0.15 inch (0.381 cm) to a length of:												
ksi	MN/m ²	0.20 in. (0.508 cm)	0.30 in. (0.762 cm)	0.40 in. (1.016 cm)	0.50 in. (1.270 cm)	0.60 in. (1.524 cm)	0.70 in. (1.778 cm)	0.80 in. (2.032 cm)	0.90 in. (2.286 cm)	1.00 in. (2.540 cm)	1.20 in. (3.048 cm)	1.40 in. (3.556 cm)	1.60 in. (4.064 cm)	1.80 in. (4.572 cm)
Temperature = 80° F (300° K)														
25	173	1,650	3,950	5,450	6,650	7,600								
15	104	4,500	11,000	15,300	18,600	21,300								
10	69	11,600	27,700	37,300	44,400	50,500	55,500	59,700	63,300	66,300				
5	35	78,000	164,000	217,000	251,000	280,000	305,000	326,000	342,000	354,000	371,000	380,000		
b ₂	14	520,000	1,630,000	2,470,000	3,000,000	3,350,000	3,630,000	3,840,000	4,010,000	4,140,000				
Temperature = 550° F (561° K)														
25	173	2,600	6,300	8,550										
15	104	5,300	13,300	19,500	24,100	28,100	30,900	33,200						
10	69	12,000	28,500	40,000	48,700	55,800	61,500							
5	35	60,000	138,000	187,000	222,000	249,000	285,000	300,000	300,000	312,000				
b ₂	14	940,000	1,760,000	2,200,000	2,510,000	2,760,000	2,970,000	3,150,000	3,410,000	3,610,000				
Temperature = -109° F (195° K)														
25	173	1,620	3,780	5,100										
15	104	4,200	10,400	14,700	18,200									
10	69													
5	35	88,000	223,000	323,000	395,000	445,000	481,000	515,000	522,000					
b ₂	14	1,850,000	3,950,000	5,150,000	5,930,000	6,420,000	6,760,000	7,080,000	7,390,000	7,680,000				

(f) PH 15-7Mo (TH 1050); $S_m = 40$ ksi (276 MN/m²)

S_a		Number of cycles required to propagate crack from length of 0.15 inch (0.381 cm) to a length of:												
ksi	MN/m ²	0.20 in. (0.508 cm)	0.30 in. (0.762 cm)	0.40 in. (1.016 cm)	0.50 in. (1.270 cm)	0.60 in. (1.524 cm)	0.70 in. (1.778 cm)	0.80 in. (2.032 cm)	0.90 in. (2.286 cm)	1.00 in. (2.540 cm)	1.20 in. (3.048 cm)	1.40 in. (3.556 cm)	1.60 in. (4.064 cm)	1.80 in. (4.572 cm)
Temperature = 80° F (300° K)														
60	414	210	390	470	510	540	550							
40	276	1,340	3,010	4,080	4,810	5,240								
20	138	4,700	10,400	13,400	14,900	15,900	16,400	17,400	17,900					
10	69	32,000	67,000	79,000	95,000	104,000	111,000	116,000	120,000	122,400	126,000	129,000		
a ₅	35	120,000	280,000	370,000	430,000	470,000	500,000	520,000	537,000	548,000	561,000	575,000		
Temperature = 550° F (561° K)														
60	414	183	323	399										
40	276	650	1,580	2,200										
20	138	3,000	6,600	8,200	9,100									
10	69	17,000	42,000	56,000	65,000	71,000	74,400	77,000						
a ₅	35	122,000	232,000	296,000	340,000	371,000	397,000	417,000	432,000	444,000	459,000	466,000		

^aCrack initiated at S_a of 10 ksi (69 MN/m²) to expedite testing.

^bCrack initiated at S_a of 5 ksi (35 MN/m²) to expedite testing.

Card 8/9

57442

Ti,SS,NiB



Card 9/9

TABLE IV.- AVERAGE CRACK PROPAGATION CHARACTERISTICS OF MATERIALS TESTED - Concluded

(g) Ti-4Al-3Mo-1V (Aged); $S_m = 25 \text{ ksi (173 MN/m}^2\text{)}$

S_a		Number of cycles required to propagate crack from length of 0.15 inch (0.381 cm) to a length of:												
ksi	MN/m^2	0.20 in. (0.508 cm)	0.30 in. (0.762 cm)	0.40 in. (1.016 cm)	0.50 in. (1.270 cm)	0.60 in. (1.524 cm)	0.70 in. (1.778 cm)	0.80 in. (2.032 cm)	0.90 in. (2.286 cm)	1.00 in. (2.540 cm)	1.20 in. (3.048 cm)	1.40 in. (3.556 cm)	1.60 in. (4.064 cm)	1.80 in. (4.572 cm)
Temperature = 80° F (300° K)														
25	173	1,360	2,210	2,770	3,000	3,150								
15	104													
10	69	7,200	16,200	22,000	25,900	29,500	32,300	34,600	36,400					
5	35	34,000	78,000	106,000	125,000	140,000	152,000	162,000	171,000	178,000				
b ₂	14	315,000	670,000	890,000	1,055,000	1,190,000	1,295,000	1,382,000	1,451,000	1,505,000	1,593,000	1,655,000	1,695,000	1,717,000
Temperature = 550° F (561° K)														
25	173	1,025	1,825											
15	104	2,800	6,800	9,300										
10	69	7,600	18,200	24,700	28,900									
5	35	74,000	130,000	165,000	187,000	201,000	210,000							
b ₂	14	480,000	1,050,000	1,410,000	1,710,000	1,940,000	2,140,000	2,310,000	2,450,000	2,570,000	2,720,000	2,820,000		

(h) Ti-6Al-4V (Annealed); $S_m = 25 \text{ ksi (173 MN/m}^2\text{)}$

S_a		Number of cycles required to propagate crack from length of 0.15 inch (0.381 cm) to a length of:												
ksi	MN/m^2	0.20 in. (0.508 cm)	0.30 in. (0.762 cm)	0.40 in. (1.016 cm)	0.50 in. (1.270 cm)	0.60 in. (1.524 cm)	0.70 in. (1.778 cm)	0.80 in. (2.032 cm)	0.90 in. (2.286 cm)	1.00 in. (2.540 cm)	1.20 in. (3.048 cm)	1.40 in. (3.556 cm)	1.60 in. (4.064 cm)	1.80 in. (4.572 cm)
Temperature = 80° F (300° K)														
25	173	1,240	2,840	3,720	4,280	4,700	5,020	5,260						
15	104	2,630	5,650	7,850	9,150									
10	69	9,000	19,400	25,600										
5	35	50,000	112,000	152,000	180,000	200,000	214,000	226,000	237,000	245,000				
b ₂	14	600,000	1,280,000	1,720,000	2,020,000	2,260,000	2,420,000	2,540,000	2,660,000	2,740,000	2,880,000	2,960,000	3,000,000	
Temperature = 550° F (561° K)														
25	173	2,500	5,450	7,000										
15	104	4,700	11,200	15,600	18,800									
10	69	9,600	22,000	30,600	37,400	42,600	47,000	51,000						
5	35	54,000	129,000	176,000	209,000	232,000	249,000	263,000	275,000	286,000	306,000	322,000	334,000	344,000
b ₂	14	360,000	930,000	1,310,000	1,600,000	1,800,000	1,970,000	2,100,000	2,230,000	2,340,000	2,520,000	2,650,000	2,740,000	2,810,000

(i) PH 14-8Mo (SRH 950); $S_m = 40 \text{ ksi (276 MN/m}^2\text{)}$

S_a		Number of cycles required to propagate crack from length of 0.15 inch (0.381 cm) to a length of:												
ksi	MN/m^2	0.20 in. (0.508 cm)	0.30 in. (0.762 cm)	0.40 in. (1.016 cm)	0.50 in. (1.270 cm)	0.60 in. (1.524 cm)	0.70 in. (1.778 cm)	0.80 in. (2.032 cm)	0.90 in. (2.286 cm)	1.00 in. (2.540 cm)	1.20 in. (3.048 cm)	1.40 in. (3.556 cm)	1.60 in. (4.064 cm)	1.80 in. (4.572 cm)
Temperature = 80° F (300° K)														
60	414	650	1,470											
40	276	1,500	3,250	4,100										
20	138	4,400	11,000	15,700	19,400									
10	69	17,500	41,000	58,000	70,000	80,000	89,000	96,800	103,500	109,000	117,000	590,000	610,000	620,000
a ₅	35	106,000	230,000	308,000	363,000	407,000	438,000	467,000	493,000	518,000	558,000	590,000	610,000	620,000
Temperature = 550° F (561° K)														
60	414	240	510											
40	276	960	2,100											
20	138	3,450	7,750	10,300										
10	69	14,000	30,800	42,500	51,000	57,500	62,500	66,200	68,600					
a ₅	35	112,000	200,000	252,000	289,000	316,000	338,000	355,000	369,000	380,000	397,000	410,000	416,000	
Temperature = -109° F (195° K)														
60	414	570	1,170	1,460										
40	276	1,760	4,120											
20	138	5,000	11,800	16,200										
10	69	32,000	65,500	86,000	102,000	111,000	119,000	124,800	129,800	134,000	140,000	723,500	731,500	
a ₅	35	169,500	390,000	497,500	567,500	612,500	642,500	662,500	680,500	704,500	710,500	723,500	731,500	

^aCrack initiated at S_a of 10 ksi (69 MN/m^2) to expedite testing.

^bCrack initiated at S_a of 5 ksi (35 MN/m^2) to expedite testing.

Ti, SS, NiB

NASA TN D-2331

Ti-8Al-1Mo-1V (Triplex Annealed) appeared to be the most resistant over the temperature range of the investigation. Special apparatus developed for the elevated- and cryogenic-temperature studies are described herein.

NASA

NASA TN D-2331

Ti-8Al-1Mo-1V (Triplex Annealed) appeared to be the most resistant over the temperature range of the investigation. Special apparatus developed for the elevated- and cryogenic-temperature studies are described herein.

NASA

NASA TN D-2331

National Aeronautics and Space Administration.
FATIGUE-CRACK PROPAGATION IN SEVERAL
TITANIUM AND STAINLESS-STEEL ALLOYS AND
ONE SUPERALLOY. C. Michael Hudson. October
1964. 30p. OTS price, \$0.75.
(NASA TECHNICAL NOTE D-2331)

Axial-load fatigue-crack-propagation tests were conducted on 8-inch-wide (20.3-cm) sheet specimens made of Ti-4Al-3Mo-1V (Aged), Ti-6Al-4V (Annealed), and Ti-8Al-1Mo-1V (Triplex Annealed) titanium alloys, AM 350 (20-percent CRT), AM 350 (Double Aged), PH 14-8Mo (SRH 950), PH 15-7Mo (TH 1050), and AISI 301 (50-percent CR) stainless steels, and René 41 (Condition B). Tests were run at 80° F (300° K), 550° F (561° K), and, in some cases, -109° F (195° K) to determine the effect of temperature on the fatigue-crack-propagation characteristics of each material. The materials are ranked according to their resistance to fatigue-crack propagation, and (over)

I. Hudson, C. Michael

II. NASA TN D-2331

NASA

NASA TN D-2331

National Aeronautics and Space Administration.
FATIGUE-CRACK PROPAGATION IN SEVERAL
TITANIUM AND STAINLESS-STEEL ALLOYS AND
ONE SUPERALLOY. C. Michael Hudson. October
1964. 30p. OTS price, \$0.75.
(NASA TECHNICAL NOTE D-2331)

Axial-load fatigue-crack-propagation tests were conducted on 8-inch-wide (20.3-cm) sheet specimens made of Ti-4Al-3Mo-1V (Aged), Ti-6Al-4V (Annealed), and Ti-8Al-1Mo-1V (Triplex Annealed) titanium alloys, AM 350 (20-percent CRT), AM 350 (Double Aged), PH 14-8Mo (SRH 950), PH 15-7Mo (TH 1050), and AISI 301 (50-percent CR) stainless steels, and René 41 (Condition B). Tests were run at 80° F (300° K), 550° F (561° K), and, in some cases, -109° F (195° K) to determine the effect of temperature on the fatigue-crack-propagation characteristics of each material. The materials are ranked according to their resistance to fatigue-crack propagation, and (over)

I. Hudson, C. Michael

II. NASA TN D-2331

NASA